OPEN

NPG Asia Materials (2017) 9, e423; doi:10.1038/am.2017.150
www.nature.com/am

ORIGINAL ARTICLE

Methemoglobin as a redox-responsive nanocarrier to trigger the *in situ* anticancer ability of artemisinin

Huan Li, Yangjun Chen, Tingting Chen, Haijie Han, Hongxin Tong, Qiao Jin and Jian Ji

Learning from the antimalarial mechanism of artemisinin (ART) in nature, we explored methemoglobin (MHb) as a smart nanocarrier of ART, in which anticancer abilities can be turned on *in situ* through the upregulated reducing capacity of tumor tissue. Ultra violet–visible, electron paramagnetic resonance spectrometry and *in vitro* cell assessment proved that a reducing agent such as glutathione can work as an excellent biogenic trigger to reduce ferric iron in MHb to the ferrous state, activating the ability of ART to generate free radicals and resulting in cytotoxicity and apoptosis. *In vivo* investigations showed that the MHb–ART complex had encouraging anticancer outcomes. The bioinspired nanocarrier may pave a new way to achieve targeted toxicity to cancer cells with extremely low side effects.

NPG Asia Materials (2017) **9,** e423; doi:10.1038/am.2017.150; published online 25 August 2017

INTRODUCTION

Artemisinin (ART) was acknowledged with the 2015 Nobel Prize in Medicine due to its great contribution to saving millions of lives from malaria.[1–3] The remarkable therapeutic effect of ART was found to arise from its endoperoxide structure, which can generate cytotoxic free radicals in the presence of ferrous iron (Fe^{2+}).[4,5] Since malarial parasites use hemoglobin as a major food source, it presents a high intracellular level of Fe^{2+} that can serve as a trigger to activate the antimalarial ability of ART.[6,7] The *in situ* trigger mechanism provides the basis of its incredibly accurate toxicity to malarial parasites with extremely low side effects.[8] Recently, the potential generation of free radicals from ART has been considered as a promising way to treat cancers,[9–11] and iron is often co-delivered with ART to enhance the free radical generation.[12,13] However, it remains challenging to develop an effective *in situ* approach to trigger free radical generation reactions within tumors. Using bio-inspiration from the antimalarial mechanism of ART in nature, here we explored methemoglobin (MHb)—an oxidized form of hemoglobin with iron in the ferric state (Fe^{3+}) rather than in the ferrous state (Fe^{2+})—as a smart nanocarrier for hydrophobic ART. While MHb reacts very slowly with ART,[14,15] the upregulated reducing capacity[16–19] of the tumor tissue can work as an excellent biogenic trigger to reduce ferric iron in MHb to the ferrous state, activating its ability to generate free radicals and resulting in the cytotoxicity of ART *in situ* (Scheme 1).

MATERIALS AND METHODS

Reagents and materials

Bovine hemoglobin and glutathione reduced ethyl ester (GSH-OEt) were purchased from Sigma-Aldrich (Shanghai, China). ART and 5,5-dimethyl-1-pyrroline 1-oxide (DMPO) were purchased from TCI (Shanghai, China), and 3-(4,5-dimethyl-thiazol-2-yl)-2,5-diphenyl tetrazolium (MTT) was purchased from YEASEN (Shanghai, China). L-glutathione (reduced) and buthionine sulfoximine (BSO) were purchased from Aladdin (Shanghai, China). The KB (human epidermoid carcinoma) cells and endothelial cells (human umbilical vein endothelial cells, 8000) were purchased from the China Center for Typical Culture Collection and Sciencell (Carlsbad, CA, USA), respectively. The endothelial cells used for the experiments underwent seven passages. All other chemicals and materials were purchased from Sinopharm Chemical Reagent (Shanghai, China) and were used as received.

Preparation of the MHb–ART complex

The 10 mg ml^{-1} bovine hemoglobin in phosphate-buffered saline (PBS) was left in the open air overnight to allow full oxidation of hemoglobin. The MHb content was determined by the Benesch equation[20] using absorbance at 560, 576 and 630 nm detected by ultra violet–visible (UV–Vis) spectrometry Shimadzu UV-2505 (Shimadzu, Tokyo, Japan). MHb with content >90% was used for further MHb–ART complex preparation. Briefly, 10 mg ml^{-1} ART in DMSO was added dropwise to a 10 mg ml^{-1} MHb solution and stirred for 30 min. The solution was transferred to an ultrafiltration centrifuge tube and washed three times by centrifugation at 4000 r.p.m. to remove the DMSO. The concentrated solution was further filtered through a sterilized 450-nm pore size filter membrane to remove any free ART. The MHb–ART complex was characterized by HT7700 transmission electron microscopy (Hitachi, Tokyo, Japan) and a Zetasizer Nano-ZS (Malvern Instruments, Malvern, UK, 633 nm He – Ne laser, 25 °C with a detection angle of 173°). To determine the amount of ART loaded in the MHb–ART complex, hydrolyzation pretreatment was performed. Briefly, 100 μl MHb–ART complex was added to 500 μl 0.2% w/w NaOH solution and incubated at 50 °C for 30 min. Then, 400 μl 0.08 M acetic acid was added to adjust the pH. The absorption at 260 nm was collected and used to determine the concentration of ART. The absorption of MHb at 260 nm after the same pretreatment should be subtracted.

Department of Polymer Science and Engineering, MOE Key Laboratory of Macromolecular Synthesis and Functionalization, Zhejiang University, Hangzhou, China
Correspondence: Professor J Ji, Department of Polymer Science and Engineering, MOE Key Laboratory of Macromolecular Synthesis and Functionalization, Zhejiang University, Zheda Road No. 38, Room 319, Hangzhou 310027, China.
E-mail: jijian@zju.edu.cn
Received 20 March 2017; revised 11 May 2017; accepted 8 June 2017

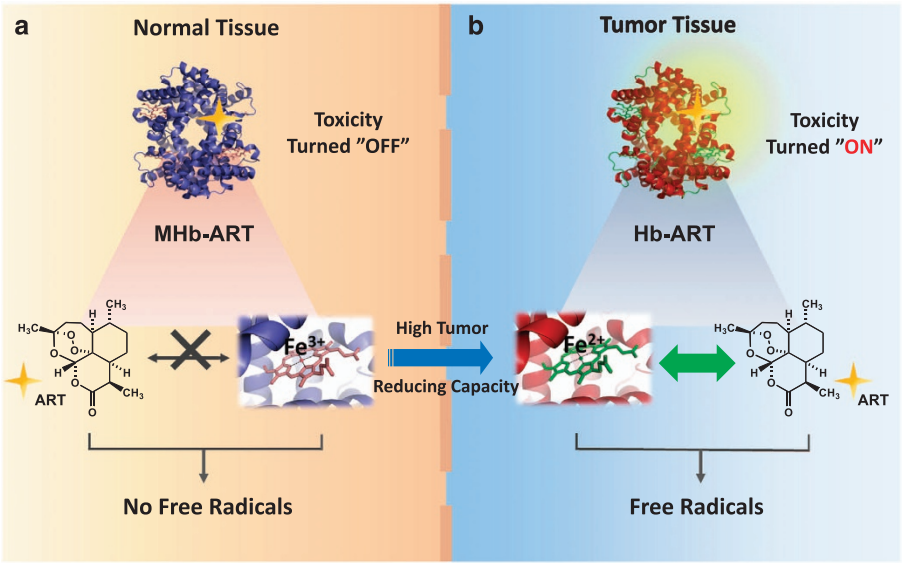

Scheme 1 Schematic diagram showing the anticancer ability of the MHb–ART complex, which can be triggered *in situ*, by relatively high reducing capacity of tumor tissue. (**a**) In normal tissue, MHb remains an inert carrier for ART because the interaction between the inner Fe^{3+} and ART negligibly generates free radicals; hence the toxicity of the MHb–ART complex is turned off. (**b**) After entering the tumor tissue, the inner Fe^{3+} of MHb can be reduced to Fe^{2+} *in situ*, triggering the interaction with ART to generate free radicals and activate the anticancer ability of the MHb–ART complex. ART, artemisinin; MHb, methemoglobin.

Redox sensitivity

UV–Vis and electron paramagnetic resonance (EPR) (BRUKER A300, Bruker, Karlsruhe, Germany) spectrometry were used to study the GSH sensitivity of the MHb–ART complex. The UV–Vis spectra were recorded immediately after adding the MHb–ART complex to a 10 mM GSH solution. EPR spectra were recorded at room temperature and operated at a frequency of 9.422513 GHz with a microwave power of 10.12 mM and field modulation of 100 kHz. The receiver gain was 3.99×10^4 and modulation amplitude was 1.00 G.

Cytotoxicity

Cytotoxicity experiments were conducted on KB cells and investigated using a standard MTT assay. KB cells were seeded into 96-well plates at 5000 cells per well and cultured at 37 °C in a humidified atmosphere with 5% CO_2 for 24 h. The cell culture medium with pH 6.5 RPMI 1640 supplemented with 10% fetal bovine serum, 100 U ml^{-1} penicillin and 100 mg ml^{-1} streptomycin to mimic the acidic microenvironment of tumor tissue. The KB cells were treated with 0.5 mM BSO for 12 h or 10 mM GSH-OEt for 2 h. Cells without pretreatment were used as a control. The cells were further treated with free ART (DMSO < 0.5%) and the MHb–ART complex at 20 μg ml^{-1} for another 24 h. The KB cells were next subjected to the MTT assay. The absorbance at 490 nm was measured using a microplate reader (MODEL 550, Bio-Rad, Hercules, CA, USA). The cell viability was obtained by comparison to blank cells treated only with the cell culture medium. The cytotoxicity of the free ART and the MHb–ART complex on endothelial cells was conducted in a similar manner, using endothelial cell medium (ECM, 1001; Sciencell) as the cell culture medium.

Apoptosis

The apoptosis assay was conducted on KB cells and investigated using an Annexin V-FITC kit (BD Company, Franklin lake, NJ, USA). KB cells were seeded into 24-well plates at 100 000 cells per well and cultured at 37 °C in a humidified atmosphere with 5% CO_2 for 24 h. The cell culture medium used here had pH 6.5 RPMI 1640 supplemented with 10% fetal bovine serum, 100 U ml^{-1} penicillin and 100 mg ml^{-1} streptomycin. The pretreatment with BSO and GSH-OEt was conducted as above. Cells were further treated with 20 μg ml^{-1} free ART (DMSO < 0.5%) or the MHb–ART complex. After double staining, the KB cells were analyzed by flow cytometry and 10 000 cells were collected.

In vivo tumor growth inhibition

Healthy male nude mice (3–4 weeks old) were purchased from the animal center at the Zhejiang Academy of Medical Sciences. Animal experiments complied with the guidelines provided by the Animal Care and Use Committee at Zhejiang University. First, 1.5×10^6 KB cells in 100 μl PBS were subcutaneously injected into the right thigh region of nude mice. All mice were ~20 g and the tumors were allowed to grow to ~65 mm^3 before experimentation. Twelve mice were randomly divided into four groups; each group contained three mice that were treated with PBS, MHb, free ART or the MHb–ART complex through tail veins every 3 days. For the free ART and MHb–ART group, the amount of intravenously injected ART was 3.00 mg kg^{-1}. Tumor size was measured every 2 days, and on day 15 all mice were killed. The tumor volume was calculated utilizing the equation: Volume = (Tumor length) × (Tumor width)^2/2.

Histology and TUNEL assay

For histology and the TUNEL assay, the major organs (heart, liver, spleen, lung and kidney) and the tumors were harvested from the mice on day 15 and were fixed in 4% neutral buffered formalin. The histology and TUNEL assay were performed by professional personnel from the medical college of Zhejiang University in a blinded fashion. The samples were examined with a microscope (Olympus BX61 inverted microscope, Olympus, Tokyo, Japan) under a bright field.

RESULTS AND DISCUSSION

Preparation of the MHb–ART complex

The self-assembled MHb–ART complex was prepared by mixing MHb (Supplementary Figure S1) and ART at a molar ratio of 1:20, referring to a previously reported strategy by Liu's group[21] with slight modifications. Dynamic light scattering results showed that the hydrodynamic size of the MHb–ART complex was 6.6 ± 0.5 nm (Supplementary Figure S2A), which is similar to the size of a single MHb.[22] This suggested that the ART molecules were encapsulated in the MHb without the formation of large complexes. Transmission electron microscopy images indicated that the MHb–ART complex was round and well-dispersed (Supplementary Figure S2B). The zeta potential of the MHb–ART complex in PBS was −9.22 ± 1.61 mV.

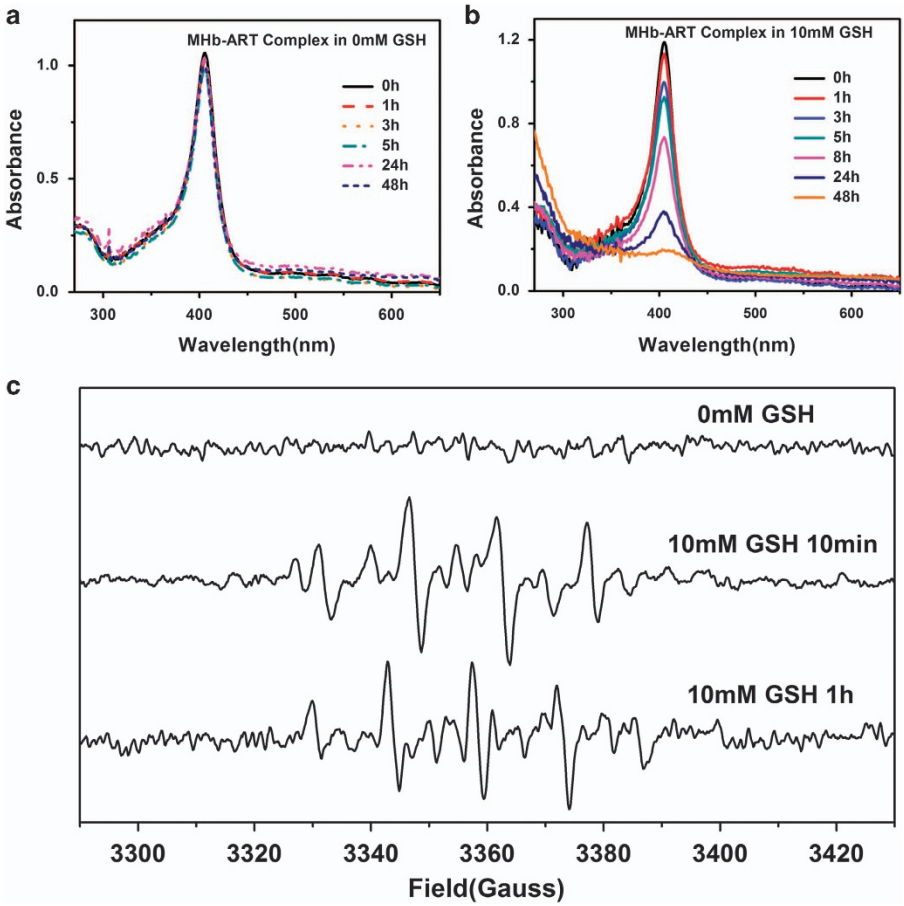

Figure 1 Redox sensitivity of the MHb–ART complex. GSH was used as a model reducing agent. UV–Vis spectra of the MHb–ART complex incubated in (**a**) 0 mM GSH solution and (**b**) 10 mM GSH solution. (**c**) EPR spectra of the MHb–ART complex in 0 mM GSH and 10 mM GSH solution. DMPO was added as a spin-trapping agent. ART, artemisinin; GSH, glutathione; MHb, methemoglobin; UV–Vis, ultra violet–visible.

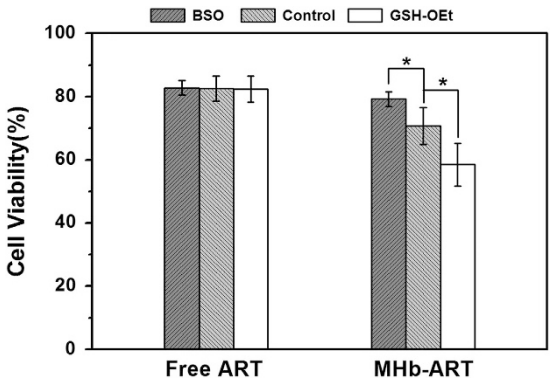

Figure 2 Cytotoxicity and GSH sensitivity of free ART and the MHb–ART complex. KB cells were treated with free ART and the MHb–ART complex for 24 h (the ART concentration was 20 μg ml^{-1}). To investigate the GSH sensitivity, cancer cells were pretreated with 0.5 mM BSO (dark gray) or 10 mM GSH-OEt (white) to suppress or promote GSH expression. The unpretreated cells (light gray) were used as a control. Data represent the mean values ± the s.d. for $n \geqslant 3$ replicates (*$P<0.05$). ART, artemisinin; BSO, buthionine sulfoximine; GSH, glutathione; GSH-OEt, glutathione reduced ethyl ester; MHb, methemoglobin; UV–Vis, ultra violet–visible.

The relatively low surface negative charge of the complex was beneficial for reducing undesirable clearance by the reticuloendothelial system and enhancing accumulation in tumor tissue.[23,24] The loading efficiency of ART in the complex was determined by UV–Vis absorption after hydrolyzation pretreatment. The molar load ratio of ART to MHb was nearly 12:1, indicating that there were three ART molecules in each hydrophobic heme pocket. The MHb–ART complex showed excellent stability (Supplementary Figure S3) and tolerable leakage (Supplementary Figure S4) in 10% serum solution, suggesting that it was suitable for further bioassays.

Redox sensitivity of the MHb–ART complex

GSH was used as a model reducing agent because it is a key reducing species in tumors and features upregulated expression in tumor cells.[25–27] UV–Vis spectrometry was applied to monitor the reaction between MHb and ART with or without GSH. It was previously reported that the reaction of ART with the iron protoporphyrin would result in a decrease in the Soret band as a consequence of disruption of the π-electron delocalization in the tetrapyrrole ring.[14] By observing the absorption of the Soret band, we learned the extent of the reaction between iron and ART. For the MHb–ART complex in 0 mM GSH, the Soret band remained nearly unchanged and only a small decrease was observed at 48 h, indicating that little hemin (Fe^{3+}) was reduced to heme (Fe^{2+}) to react with ART (Figure 1a). By contrast, for the MHb–ART complex in 10 mM GSH, the Soret band decreased significantly over time and barely any unreacted hemin remained at 48 h (Figure 1b). This meant that GSH could work as a reducing agent to transform the hemin in MHb to heme, thereby activating its ability to interact with ART.

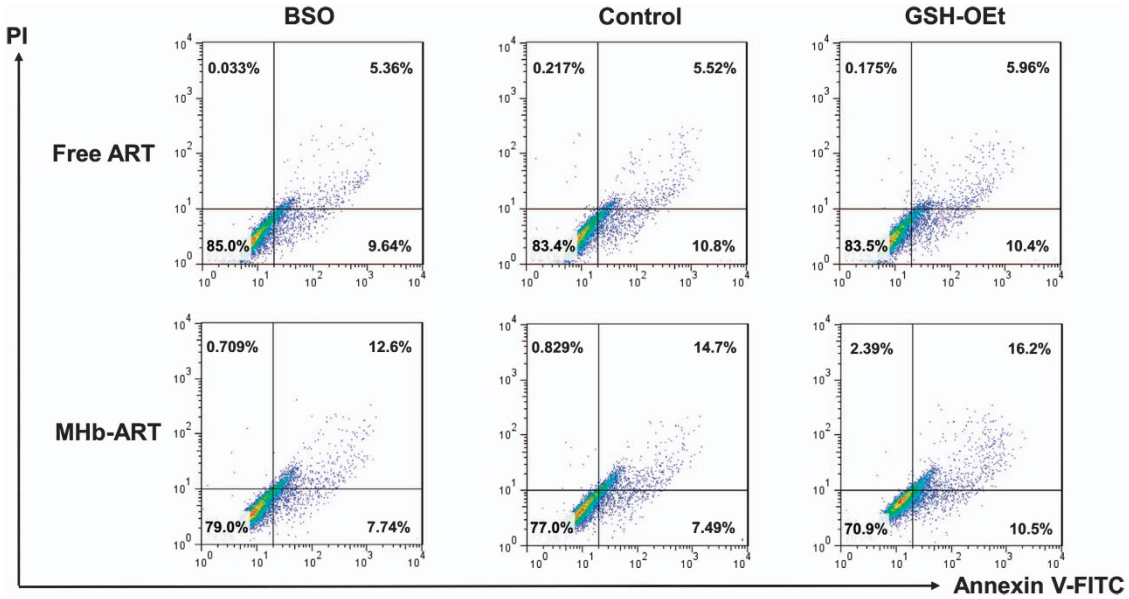

Figure 3 Apoptosis of KB cells treated with free ART or the MHb–ART complex. The concentration of ART was 20 μg ml^{-1}. To assess the role of GSH, KB cells were pretreated with 0.5 mM BSO or 10 mM GSH-OEt, and unpretreated cells were used as a control. ART, artemisinin; BSO, buthionine sulfoximine; GSH, glutathione; GSH-OEt, glutathione reduced ethyl ester; MHb, methemoglobin.

EPR spectrometry was further utilized to obtain direct information about the free radical generation of the MHb–ART complex in a reducing environment, using DMPO as a spin-trapping agent. The EPR spectra (Figure 1c) showed that the MHb–ART complex alone did not generate free radicals, making them safe candidates for normal tissues with relatively low GSH levels. After a 10 min addition of the MHb–ART complex to 10 mM GSH, a typical DMPO-OH adduct spectrum was detected, implying that the hydroxyl radical (•OH) was generated from the MHb–ART complex by adding GSH. After 1 h addition of the MHb–ART complex to 10 mM GSH, the EPR spectrum changed dramatically with the signal, mainly due to the DMPO adduct of carbon-centered free radicals (Supplementary Figure S5). This was in accordance with the widely accepted fact that oxygen radicals generated by ART subsequently rearrange into carbon-centered radicals.[28,29] Together, these results confirmed the ability of GSH to reduce the ferric iron in MHb to a ferrous state to activate the potential of ART to generate free radicals.

Cytotoxicity

The cytotoxicity of free ART and the MHb–ART complex to KB cells (human epidermoid carcinoma) was studied *in vitro* using a standard MTT assay. As shown in Figure 2 (light gray group), the MHb–ART complex showed higher cytotoxicity to cancer cells than free ART, which could be attributed to the iron-enhancing effect of the MHb nanocarrier. In the presence of reducing agents such as GSH, MHb could be reduced *in situ* and work as an additional Fe^{2+} source to increase the iron-mediated free radical generation of ART, while free ART merely relied on the intrinsic Fe^{2+} of cancer cells to generate toxic radicals. That is, the MHb–ART complex exhibited more encouraging anticancer ability than free ART. The MHb nanocarrier itself showed no cytotoxicity to KB cells (Supplementary Figure S6), indicating that cell death was the result of the interaction between ART and the nanocarrier. The MHb–ART complex was further proved to exhibit dose-dependent cytotoxicity (Supplementary Figure S7). In addition, similar to free ART, no obvious cytotoxicity was observed when treating normal cells such as endothelial cells with the MHb–ART complex (Supplementary Figure S8), implying the safety of utilizing MHb as an iron-supplying nanocarrier.

To further evaluate the role of GSH in triggering cytotoxicity, we suppressed or promoted the expression levels of GSH in KB cells and observed the influence of GSH on the cytotoxicity of free ART and the MHb–ART complex. BSO and GSH-OEt were used to pretreat KB cells for 12 and 2 h separately to suppress or enhance the GSH levels inside the KB cells. Cancer cell without pretreatment was used as a control. As shown in Figure 3, for KB cells treated with free ART, there was little difference among the control groups and those pretreated with BSO or GSH-OEt. This implied that GSH did not significantly affect the cytotoxicity of free ART, whose toxicity merely relied on the intracellular levels of Fe^{2+}. For KB cells treated with the MHb–ART complex, BSO pretreatment significantly enhanced the cell viability, while GSH-OEt pretreatment distinctly decreased the cell viability over the control group. This verified the ability of GSH to trigger the anticancer ability of the MHb–ART complex.

Apoptosis

Apoptosis is a commonly reported effect that ART-related drugs exert on cancer cells.[9,11,30] Herein, the potency of free ART and MHb–ART in inducing cancer cell apoptosis was studied. As seen in Figure 3, when the KB cells were treated with the MHb–ART complex, the total cell population of the early and late apoptosis state was significantly higher than for the free ART group. In particular, the proportion of late apoptosis cells was approximately three-fold higher in the MHb–ART group (14.7%) than the free ART group (5.52%), showing the enhanced potency of the MHb–ART complex in inducing apoptosis. This was in agreement with the results of the inhibition of cancer cell proliferation (Figure 2) and can be attributed to the complement of iron supplied by MHb nanocarriers. The BSO and GSH-OEt pretreatments were applied again to study the effect of GSH on the apoptosis-inducing ability. When exposed to free ART, there was no significant difference in apoptosis between the pretreated KB cells and the control cells. This suggested that GSH was not crucial in free ART-induced apoptosis. For KB cells treated with the MHb–ART complex,

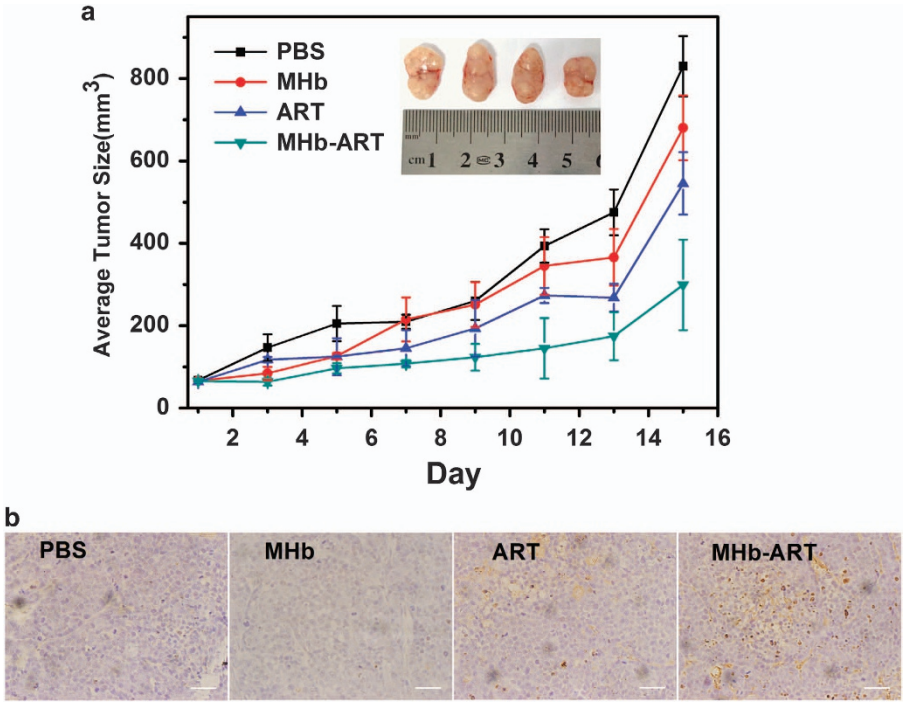

Figure 4 *In vivo* anticancer investigation. (**a**) Anticancer ability of PBS, MHb, free ART and the MHb–ART complex, respectively. The inset shows a digital image of tumors harvested on day 15 (from left to right are tumors treated with PBS, MHb, ART and the MHb–ART complex, respectively). (**b**) TUNEL assay of the tumors harvested on day 15. Scale bars: 50 μm. ART, artemisinin; MHb, methemoglobin; PBS, phosphate-buffered saline.

the proportion of apoptosis cells gradually increased among the BSO-treated cells (20.3%), control cells (22.2%) and GSH-OEt-treated cells (26.7%), which is indicative of the key role of GSH in turning on the ability of the complex to induce apoptosis. Interestingly, even when the GSH expression level of the KB cells was suppressed by BSO, the apoptosis cell population of KB cells treated with the MHB–ART complex was still higher than cells treated with free ART. This was because there are other reducing agents in addition to GSH such as thioredoxin,[31] cysteine[32] and homocysteine[33] inside cancer cells, which can work as a trigger to provoke the anticancer ability of the MHb–ART complex.

In vivo assessment

We further studied the efficacy of the *in vivo* tumor inhibition of the MHb–ART complex. Healthy male nude mice bearing KB tumors were treated with PBS, MHb, free ART and the MHb–ART complex, respectively. All four groups showed an increase in tumor size with time, but tumor growth was maximally suppressed in mice treated with the MHb–ART complex (Figure 4a). Once again, this shows that as an *in situ* translated Fe^{2+} source, the MHb nanocarrier could distinctly enhance the anticancer ability of the complex. The TUNEL assay was conducted on tumors harvested on day 15 to study whether there was any apoptosis inside the tumor tissues (Figure 4b). Little apoptosis was observed in tumor tissue treated with PBS or MHb. For mice treated with free ART and the MHb–ART complex, all showed TUNEL-positive brown areas but the MHb–ART complex group showed significantly more apoptosis. This was in agreement with the apoptosis-inducing potency of the previously studied free ART and the MHb–ART complex (Figure 3) and is attributed to the antitumor ability. To gain more insight into the potential influence of the MHb–ART complex on major organs, we performed H&E staining assays (Supplementary Figure S9). No obvious pathological abnormalities were observed in the major organs including heart, liver, spleen, lung and kidney for all four groups. Along with the low toxicity of the MHb–ART complex on normal cells such as endothelial cells (Supplementary Figure S4), the MHb encapsulation of ART can indeed be deemed an effective way to prevent the pre-interaction between ART and iron to generate toxic free radicals. Histological examination of tumor tissues (Supplementary Figure S9) showed that tumor tissues from the PBS and MHb groups were abundant with cancer cells with no obvious damage. For the free ART group, significant damage to tumor tissues began to arise. In the MHb–ART complex group, massive cell death and damage were observed in the tumor tissues, further confirming the anticancer ability of the MHb–ART complex. All of the above *in vivo* anticancer investments showed that the MHb–ART complex is a promising anticancer agent with few side effects and a potent ability to suppress tumor growth.

CONCLUSION

On the basis of the natural mechanism underlying the antimalarial ability of ART, we developed the potential of MHb as a redox-responsive nanocarrier that could be applied to other lethal disease treatments such as for cancer. The encapsulation of ART into the MHb nanocarrier enabled iron-mediated free radical generation to be triggered *in situ* through an elevated tumor-reducing capacity. UV–Vis and EPR spectrometry, along with *in vitro* cell evaluations, have confirmed the iron-enhancing role and redox sensitivity of the MHb nanocarrier. The *in vivo* assessments further proved the promising anticancer ability of the MHb–ART complex. In principle, the MHb–ART complex could be utilized in any life-threatening disease with a prominent reducing environment. More importantly, this work could pave a new way to tackle the dilemma of developing efficient pharmaceutical agents with few side effects.

CONFLICT OF INTEREST

The authors declare no conflict of interest.

ACKNOWLEDGEMENTS

Financial support from the National Science Fund (NSFC-21574114 and 51333005) is gratefully acknowledged.

PUBLISHER'S NOTE

Springer Nature remains neutral with regard to jurisdictional claims in published maps and institutional affiliations.

1 Klayman, D. L. Qinghaosu (artemisinin): an antimalarial drug from China. *Science* **228**, 1049–1055 (1985).
2 Tu, Y. Artemisinin-a gift from traditional Chinese medicine to the world (Nobel Lecture). *Angew. Chem. Int. Ed.* **55**, 10210–10226 (2016).
3 Bhatt, S., Weiss, D. J., Cameron, E., Bisanzio, D., Mappin, B., Dalrymple, U., Battle, K. E., Moyes, C. L., Henry, A. & Eckhoff, P. A. The effect of malaria control on *Plasmodium falciparum* in Africa between 2000 and 2015. *Nature* **526**, 207–211 (2015).
4 Golenser, J., Waknine, J. H., Krugliak, M., Hunt, N. H. & Grau, G. E. Current perspectives on the mechanism of action of artemisinins. *Int. J. Parasitol.* **36**, 1427–1441 (2007).
5 Wu, W., Wu, Y., Wu, Y., Yao, Z., Zhou, C., Li, Y. & Shan, F. Unified mechanistic framework for the Fe(II)-induced cleavage of Qinghaosu and derivatives/analogues. The first spin-trapping evidence for the previously postulated secondary C-4 radical. *J. Am. Chem. Soc.* **120**, 3316–3325 (1998).
6 Elliott, D. A., Mcintosh, M. T., Chen, S., Zhang, G., Baevova, P. & Joiner, K. A. Four distinct pathways of hemoglobin uptake in the malaria parasite *Plasmodium falciparum*. *Proc. Natl Acad. Sci. USA* **105**, 2463–2468 (2008).
7 Wang, J., Zhang, C. J., Ni, C. W., Loh, C. C. Y., Li, Z., Mun, L. Y., He, Y., Yuan, L. X., Kwang, L. T. & Min, L. Haem-activated promiscuous targeting of artemisinin in *Plasmodium falciparum*. *Nat. Commun.* **6**, 10111 (2015).
8 Meshnick, S. R. Artemisinin: mechanisms of action, resistance and toxicity. *Int. J. Parasitol.* **32**, 1655–1660 (2002).
9 Zhang, C. J., Wang, J., Zhang, J., Lee, Y. M., Feng, G., Lim, T. K., Shen, H. M., Lin, Q. & Liu, B. Mechanism-guided design and synthesis of a mitochondria-targeting artemisinin analogue with enhanced anticancer activity. *Angew. Chem. Int. Ed.* **55**, 13770–13774 (2016).
10 Tilaoui, M., Mouse, H. A., Jaafari, A. & Zyad, A. Differential effect of artemisinin against cancer cell lines. *Nat. Prod. Bioprospect.* **4**, 189–196 (2014).
11 Chaturvedi, D., Goswami, A., Saikia, P. P., Barua, N. C. & Rao, P. G. Artemisinin and its derivatives: a novel class of anti-malarial and anti-cancer agents. *Chem. Soc. Rev.* **41**, 435–454 (2010).
12 Zhang, H., Lin, H., Jiao, X., Ji, Y., Zhu, X. & Zhang, Z. Transferrin-mediated fullerenes nanoparticles as Fe^{2+} -dependent drug vehicles for synergistic anti-tumor efficacy. *Biomaterials* **37**, 353–366 (2014).
13 Efferth, T., Benakis, A., Romero, M. R., Tomicic, M., Rauh, R., Steinbach, D., Häfer, R., Stamminger, T., Oesch, F. & Kaina, B. Enhancement of cytotoxicity of artemisinins toward cancer cells by ferrous iron. *Free Radic. Biol. Med.* **37**, 998–1009 (2004).
14 Messori, L., Gabbiani, C., Casini, A., Siragusa, M., Vincieri, F. F. & Bilia, A. R. The reaction of artemisinins with hemoglobin: a unified picture. *Bioorg. Med. Chem.* **14**, 2972–2977 (2006).
15 Zhang, S. & Gerhard, G. S. Heme activates artemisinin more efficiently than hemin, inorganic iron, or hemoglobin. *Bioorg. Med. Chem.* **16**, 7853–7861 (2008).
16 Khramtsov, V. V. & Gillies, R. J. Janus-faced tumor microenvironment and redox. *Antioxid. Redox Signal.* **21**, 723–729 (2014).
17 Bobko, A. A., Eubank, T. D., Voorhees, J. L., Efimova, O. V., Kirilyuk, I. A., Petryakov, S., Trofimiov, D. G., Marsh, C. B., Zweier, J. L., Grigor'ev, I. A., Samouilov, A & Khramtsov, V. V. *In vivo* monitoring of pH, redox status, and glutathione using L-band EPR for assessment of therapeutic effectiveness in solid tumors. *Magn. Reson. Med.* **67**, 1827–1836 (2012).
18 Wang, J., Sun, X., Mao, W., Sun, W., Tang, J., Sui, M., Shen, Y. & Gu, Z. Tumor redox heterogeneity-responsive prodrug nanocapsules for cancer chemotherapy. *Adv. Mater.* **25**, 3670–3676 (2013).
19 Sun, H., Meng, F., Cheng, R., Deng, C. & Zhong, Z. Reduction-responsive polymeric micelles and vesicles for triggered intracellular drug release. *Antioxid. Redox Signal.* **21**, 755–767 (2013).
20 Benesch, R. E., Benesch, R. & Yung, S. Equations for the spectrophotometric analysis of hemoglobin mixtures. *Anal. Biochem.* **55**, 245–248 (1973).
21 Chen, Q., Wang, C., Zhan, Z., He, W., Cheng, Z., Li, Y. & Liu, Z. Near-infrared dye bound albumin with separated imaging and therapy wavelength channels for imaging-guided photothermal therapy. *Biomaterials* **35**, 8206–8214 (2014).
22 Milsom, E. V., Dash, H. A., Jenkins, T. A., Opallo, M. & Marken, F. The effects of conductivity and electrochemical doping on the reduction of methemoglobin immobilized in nanoparticulate TiO2 films. *Bioelectrochemistry* **70**, 221–227 (2007).
23 Xiao, K., Li, Y., Luo, J., Lee, J. S., Xiao, W., Gonik, A. M., Agarwal, R. G. & Lam, K. S. The effect of surface charge on *in vivo* biodistribution of PEG-oligocholic acid based micellar nanoparticles. *Biomaterials* **32**, 3435–3446 (2011).
24 Li, J., Yu, X., Wang, Y., Yuan, Y., Xiao, H., Cheng, D. & Shuai, X. A reduction and pH dual-sensitive polymeric vector for long-circulating and tumor-targeted siRNA delivery. *Adv. Mater.* **26**, 8217–8224 (2014).
25 Kuppusamy, P., Li, H., Ilangovan, G., Cardounel, A. J., Zweier, J. L., Yamada, K., Krishna, M. C. & Mitchell, J. B. Noninvasive imaging of tumor redox status and its modification by tissue glutathione levels. *Cancer Res.* **62**, 307–312 (2002).
26 Russo, A., Degraff, W., Friedman, N. & Mitchell, J. B. Selective modulation of glutathione levels in human normal versus tumor cells and subsequent differential response to chemotherapy drugs. *Cancer Res.* **46**, 2845–2848 (1986).
27 Wong, Y. K., Hsiao, Y. L., Poon, C. K., Kwan, P. C., Chao, S. Y., Chou, S. T. & Yang, C. S. Glutathione concentration in oral cancer tissues. *Cancer Lett.* **81**, 111–116 (1994).
28 Posner, G. H. & O'Neill, P. M. Knowledge of the proposed chemical mechanism of action and cytochrome p450 metabolism of antimalarial trioxanes such as artemisinin allows rational design of new antimalarial peroxides. *Acc. Chem. Res.* **37**, 397–404 (2004).
29 O'Neill, P. M., Barton, V. E. & Ward, S. A. The molecular mechanism of action of artemisinin-the debate continues. *Molecules* **15**, 1705–1721 (2010).
30 Min, L. W. Targeting apoptosis pathways in cancer by Chinese medicine. *Cancer Lett.* **332**, 304–312 (2013).
31 Lillig, C. H. & Holmgren, A. Thioredoxin and related molecules–from biology to health and disease. *Antioxid. Redox Signal.* **9**, 25–47 (2007).
32 Koch, C. J. & Evans, S. M. Cysteine concentrations in rodent tumors: unexpectedly high values may cause therapy resistance. *Int. J. Cancer* **67**, 661–667 (1996).
33 Hultberg, B., Andersson, A. & Isaksson, A. The effects of homocysteine and copper ions on the concentration and redox status of thiols in cell line cultures. *Clin. Chim. Acta* **262**, 39–51 (1997).

This work is licensed under a Creative Commons Attribution 4.0 International License. The images or other third party material in this article are included in the article's Creative Commons license, unless indicated otherwise in the credit line; if the material is not included under the Creative Commons license, users will need to obtain permission from the license holder to reproduce the material. To view a copy of this license, visit http://creativecommons.org/licenses/by/4.0/

© The Author(s) 2017

Supplementary Information accompanies the paper on the NPG Asia Materials website (http://www.nature.com/am)